



Textural Properties Characterization for NaX and FeX Zeolites by Nitrogen Adsorption-desorption Technique

Sanarya K. Kamal and Ammar S. Abbas

Chemical Engineering Department, College of Engineering, University of Baghdad, Baghdad, Iraq

Abstract

The zeolite's textural properties have a significant effect on zeolite's effectiveness in the different industrial processes. This research aimed to study the textural properties of the NaX and FeX zeolites using the nitrogen adsorption-desorption technique at a constant low temperature. According to the International Union of Pure and Applied Chemistry, the adsorption-desorption isotherm showed that the studied materials were mixed kinds I/II isotherms and H3 type hysteresis. The Brunauer-Emmett-Teller isotherm was the best model to describe the nitrogen adsorption-desorption better than the Langmuir and Freundlich isotherms. The obtained adsorption capacity and Brunauer-Emmett-Teller surface area values for NaX were greater than FeX. According to the Kelvin equation, Barrett, Joyner, and Halenda model was used to determine pore size distribution, diameter, and average pore volume for the selected zeolites. The pore size distribution for NaX was wider than FeX zeolites, the pore diameter for NaX was less than FeX, and the average pore volume for FeX was greater than the value of NaX average pore volume. The comparative study was carried out with the previous studies, and the comparison showed that the textural properties of the modified zeolites agreed with other studies.

Keywords: ion-exchange; mesoporous; pore size distribution; surface area; pore diameter; isotherms; average pore volume.

Received on 15/06/2022, Accepted on 10/09/2022, Published on 30/12/2022

<https://doi.org/10.31699/IJCPE.2022.4.5>

1- Introduction

A zeolite mineral is a crystalline substance made of interconnected tetrahedra, each of which has four O atoms around a cation. Zeolite system has open voids in the shape of channels and cages [1]. Zeolite type X are microporous crystalline minerals composed of oxygen-bonded SiO₄ and AlO₄ tetrahedra. The negative charge in the zeolite framework is balanced by exchangeable cations [2].

Using zeolites is expanded by modifying them. Ion-exchange reactions can dramatically alter the surface characteristics of zeolites when using cationic surfactants [3], and it is essential to adjust ion-exchange materials' chemical structure and content using proper pretreatment. To enhance ion-exchange capabilities and obtain a porous substance with a high absorption capacity, it must also have a significant specific area, displaying a porous structure with micropores. Water and exchangeable cations may fill zeolite's crystal and porous form, which has a particular pore size [4]. Zeolites are widely employed in a wide range of applications; they can be used as adsorbents [5-7], sorbents for dyes [8,9], heavy metals [10], and other contaminants in wastewater and natural water [11], molecular filter [12], ion-exchange compounds [13,14], catalyst [15-17]. The textural properties of zeolites significantly affect their effectiveness in industrial processes. Thus, studying the porous materials' textural properties by the nitrogen

adsorption-desorption technique is essential. The textural properties include the pore size distribution, surface area (S_{BET}), pore diameter (d_{BJH}), and average pore volume (V_p).

The gas adsorption process is a typical process for describing porous solids. The nitrogen adsorption-desorption method measures materials' S_{BET} and pore size distribution [18,19]. Adsorption is a surface process that defines the interaction between two distinct phases that results in the formation of an interface layer by transferring a molecule from a fluid bulk (liquid or gas) (adsorbate) to a solid surface (adsorbent) [20,21].

The gas adsorbed in a solid depends upon the surface area where the larger surface area of the adsorbent will be active site, so the rate of adsorption increases, temperature, the pressure of the gas, and the gas nature. The adsorption isotherm is the relationship between the adsorbate in the liquid phase and the adsorbent's surface at equilibrium at a specific temperature [22,23]. The International Union of Pure and Applied Chemistry (IUPAC) divides adsorption isotherms into six types depending on the shape of the isotherm of relative pressure and the gas adsorbed onto a solid surface [24]. The first category I isotherms shows monolayer adsorption. Pore size is not significantly more significant than the molecular diameter of the adsorbate molecules. The adsorption increases with pressure until it reaches saturation. Hence, no further adsorption occurs regarding the second category II, often known as macro-porous

adsorbents, which have a wide variety of pore diameters, obtained when the bilayer is created after the monolayer is complete. The tri-layer is generated after the bilayer is full. The third category (III), the adsorption isotherm, is obtained when the monolayer formation is followed by multilayer the adsorption quantity increases virtually exponentially. In the fourth category (IV), the lower pressure region is like the category II isotherm, which clarifies the formation of monolayer followed by multilayer on the pore wall much more comprehensive than the sorbate molecular diameter (mesoporous). The fifth category (V) adsorption isotherm is like category IV when intermolecular attraction effects are strong, and adsorption occurs in pores. Finally, the sixth category (VI) isotherm signifies layer-by-layer adsorption on a nonporous surface with substantial uniformity. The capacity of each adsorbed layer is represented by the step height, while the step sharpness depends on the system and temperature [22,25]. Carbon dioxide, argon, and nitrogen are gases that may be used for adsorption-desorption (N_2). N_2 (measured at 77.35 K) has remained extensively familiar and regarded as friendly commercial apparatus between these many gases and vapors existing and might be employed as adsorbate [24]. Various adsorption models are used to describe adsorption isotherms experimental data for different porous materials [18, 26-30].

This research investigated the textural properties of NaX zeolite, and its modified version by Fe (II) exchanged (FeX) using N_2 adsorption-desorption technique. The obtained data would be fitted with different adsorption isotherms. The Brunauer-Emmett-Teller (BET) would obtain the S_{BET} . Finally, the Barrett-Joyner-Halenda (BJH) will get pore size distribution, d_{BJH} , and V_p . The obtained results will be compared with the previous studies.

2- Experimental

2.1. Preparation of Fe (II) ion-exchanged zeolite (FeX)

NaX zeolite (commercial grain) was crushed and then sieved with 200 mesh strainers to homogenize the size. NaX zeolite containing a high sodium weight percentage (14.719%) was exposed to an ion-exchange procedure with ferrous sulfate heptahydrate ($FeSO_4 \cdot 7H_2O$, India) to replace the sodium from NaX zeolite. 5 g of dried NaX zeolite was added to 100 ml of a 0.319 M solution and maintained at controlled temperatures of 80°C with constant stirring (300 rpm) for 8 hours. Then exchanged NaX zeolite samples were taken from the ion-exchanged solution and filtered, washed several times with distilled water to remove the Fe (II), which had not been exchanged, and taken to an oven for drying overnight at 60 °C overnight. The sample was calcined in a furnace at 550 °C for 3 hours; then, it was left to cool inside in a desiccator until it reached room temperature.

The concentration of Fe (II) in the exchange solution was measured using atomic absorption spectrophotometry (VarianAA240FS, Australia), and the amount of exchange

Fe (II) was determined. The atomic absorption spectrophotometry was tested at North Gas Company (Ministry of Oil, Iraq).

2.2. Adsorption-desorption tests

N_2 adsorption-desorption occurred over samples of NaX zeolite (0.0779 g), and FeX zeolite (0.2047 g) were measured using the Micromeritics ASAP 2020 instrument. All tests were accomplished at the Petroleum Research and Development Center, Ministry of Oil (Iraq). After performing each measurement three times, the average values of the obtained data were calculated, recorded, and afterward utilized in the investigation of the isotherm models. After that, measurements were taken to determine the S_{BET} , particle size distribution, pore diameter, and V_p values.

2.3. Langmuir isotherm model

Langmuir explained the isotherm model, primarily designed to describe gases adsorbed to solid and obtained in 1916 [31]. Langmuir model assumes that the adsorption consists of a monolayer at the surface, and no further adsorption occurs. The adsorbent's surface is homogenous [20,32]. The Langmuir isotherm is expressed as in Eq. (1).

$$\frac{P}{Q} = \frac{P}{Q_m} + \frac{1}{Q_m K_L} \quad (1)$$

K_L can be associated with the difference in the adsorbent's porosity and suitable area, indicating that a higher pore volume and surface area will result in a higher adsorption capacity [33]. A plot of P/Q against P should give a straight line with slope $\frac{1}{Q_m}$ and intercept $\frac{1}{Q_m K_L}$ and find the Langmuir constant and the monolayer maximum sorption capacity [31].

2.4. Freundlich isotherm model

Freundlich isotherm is an empirical equation published in 1906 and extensively applied to model the multilayer adsorbed on heterogeneous surfaces at a specific temperature [34]. Freundlich model equation represents in Eq. (2) [35].

$$\text{Log}Q = \text{Log}K_f + \frac{1}{n} \text{Log}P \quad (2)$$

2.5. BET isotherm model

A significant application of the BET isotherm is the surface area measurement for solid materials. The surface area can be approximated by utilizing the BET equation derived from a specific region of a gas adsorption isotherm. After the BET theory's publication, this area on

the isotherm is where gas monolayers are thought to develop [36]. The BET theory relies significantly on the concept that the surface of a substance can play presenter to the adsorption of gases. The BET study is predicated on the adsorption isotherms of nonreactive gas molecules, such as nitrogen or argon, at a pressure range that encompasses the monolayer coverage of molecules [37]. An example of a theoretical equation that can compute the surface area of gas-solid equilibrium systems is the BET isotherm, which can be found [38].

$$\frac{\left(\frac{P}{P^o}\right)}{Q\left[1-\left(\frac{P}{P^o}\right)\right]} = \frac{C-1}{Q_m C} \left(\frac{P}{P^o}\right) + \frac{1}{Q_m C} \quad (3)$$

Where C relates to the difference between the heat of adsorption in the first layer (E_1) and the heat of vaporization (E_L) = $\exp\left(\frac{E_1 - E_L}{RT}\right)$ [25], the nitrogen adsorption data obtained in the current investigation could be used only using a limited range of relative pressures (0.05-0.3) or, in many cases, up to 0.4 [39]. In that state, the linear plot between the term $\left(\frac{P}{P^o}\right) / \left(Q\left[1-\left(\frac{P}{P^o}\right)\right]\right)$ and relative pressure $\left(\frac{P}{P^o}\right)$ allows determining Q_m and C from intercept and slop. After calculating these values, the total surface area (S_t), may be computed using the value of Q_m [39].

2.6. Determination of the total surface area

The total surface area of samples was verified using Eq. (4) [40].

$$S_t = \frac{Q_m NA_m}{V} \quad (4)$$

In the adsorption, the N_2 molecule cross-sectional area equals 0.1620 nm^2 , nitrogen absorbed molar volume (22.414 L/mole).

2.7. BJH pore diameter and volume

(BJH) is a method used for measuring pore size distribution and pore volume from experimental data. Using the data from the N_2 adsorption-desorption isotherm at 77.35 K , it is possible to determine both the d_{BJH} and the V_p of the adsorbent. BJH improved in 1951 [41] by imagining that all pore shapes are cylindrical with nonintersecting and open ends. BJH model presumed that the pore radius was equal to the combination of the Kelvin radius and the thickness of the adsorbed layer, as found in the Eq. (5) [42].

$$\ln\left(\frac{P}{P^o}\right) = -\frac{C\gamma v \cos \theta}{RT(r-t)} \quad (5)$$

The Halsey equation may calculate the thickness of the adsorbed layer remain on the pore walls as shown in Eq. (6) [43].

$$t = 3.54 \left(\frac{-5}{\ln\left(\frac{P}{P^o}\right)} \right)^{0.333} \quad (6)$$

3- Results and Discussion

The findings on N_2 adsorption-desorption were utilized to determine the kind of the isotherm and the nature of the adsorption process for chosen zeolites. Fig. 1 showed the N_2 adsorption-desorption isotherms on the NaX and FeX zeolites surfaces. The curves displayed that the micropore filling was noticed at a proportionally low pressure owing to the narrow pore width and the excellent adsorption potential, the phenomenon refers to the category I isotherm for the microporous materials. The adsorption increases with pressure until it reaches saturation. Whereas at $P/P^o \geq 0.8$ suggests pore expansion; mesopore adsorption played a role in the adsorption process, the phenomenon refers to category II isotherm characteristics. The NaX had micropores and mesopores, but following the ion-exchange, the volume of N_2 adsorbed at low P/P^o values dropped, implying a reduction in available microporosity. The findings indicated that the adsorption isotherms combined the kinds I/II. In Fig. 1 (a), the quantity of N_2 absorbed by NaX zeolite was $230.11 \text{ cm}^3/\text{g}$, while the FeX only absorbed $184.84 \text{ cm}^3/\text{g}$, as displayed in Fig. 1 (b). According to the IUPAC category, the NaX and FeX zeolites, mesoporous materials, could be categorized as mixed kinds I/II isotherms and H3 type hysteresis based on the adsorption-desorption data forms at 77.35 K [25,44].

The microporous adsorption contribution in FeX zeolite was lower than in NaX zeolite due to Fe exchange on zeolite, so the surface of the zeolite became more porous and rougher. Demonstrating this the fact that the slope of the region in the middle of the desorption isotherm curves of the NaX zeolites increased after Fe (II) exchanges were placed.

Fig. 1 (b) showed nitrogen adsorption/desorption on FeX at 77.35 K ; the hysteresis loop for nitrogen adsorption on the sample closed at a relative pressure of $4.0-4.5$ [25], indicating small mesopores, as shown in the figure. The hysteresis stayed open longer, but the nitrogen meniscus failed due to tensile strength failure; hysteresis (type H3) demonstrates capillary condensation in mesopores by the IUPAC [25]. The initial steep slope indicates where monolayer formation was most likely to occur. The first few multilayers can be seen in the middle of the isotherm's low slope zone.

The Langmuir, Freundlich, and BET isotherm models were employed to explain the experimental results of N_2 adsorption on the surface of NaX and FeX zeolites. Fig. 2 to Fig. 4 illustrate the NaX zeolite and FeX isotherm models. Langmuir isotherm model shown as Eq. 1 in Fig. 2 was displayed for NaX and FeX zeolites. The isotherm model was a better fit for the N_2 adsorption data for the NaX zeolite (Fig. 2, a) with a correlation value (R^2) of 0.9999, while the correlation coefficient (R^2) for the FeX zeolite was 0.9978 (Fig. 2, b).

Both the NaX and FeX adsorption data were well represented by the Freundlich isotherm model (Eq. 2), as shown in Fig. 3, with correlation coefficients R^2 equal to 0.9961 for NaX zeolite and 0.9929 for FeX. The BET isotherm model (Eq. 3) correctly fitted the N_2 adsorption data for both mesoporous, with correlation coefficient (R^2) equal to 0.9914 and 0.9996, for NaX zeolite and FeX, respectively. Table 1 shows the regression coefficients

and fitted constants for NaX zeolite and FeX isotherm models.

According to the BET isotherm model, NaX zeolite had an adsorption capacity of $188.39 \text{ cm}^3/\text{g}$, while FeX had an adsorption capacity of $68.05 \text{ cm}^3/\text{g}$. The surface area of NaX zeolite and FeX was calculated using the BET model (Eq. 4), and found after the ion-exchange process, the surface area decreased from $569.14 \text{ m}^2/\text{g}$ and $213.31 \text{ m}^2/\text{g}$, respectively. Fig. 5 the pore size distribution for the examined mesoporous adsorbents was calculated using the BJH model and N_2 adsorption data at 77.35 K NaX and FeX zeolites. NaX had a wider pore size distribution (Fig. 5, a) than FeX (Fig. 5, b). The peaks of the two materials' pore size distribution (mode pore size diameter) were 2.45 nm for NaX and 5.19 nm for FeX. NaX had a total pore volume of $0.349 \text{ cm}^3/\text{g}$, while FeX had a total pore volume of $5.190 \text{ cm}^3/\text{g}$. The ion-exchange process appears to impact characteristics such as surface area and pore volume significantly.

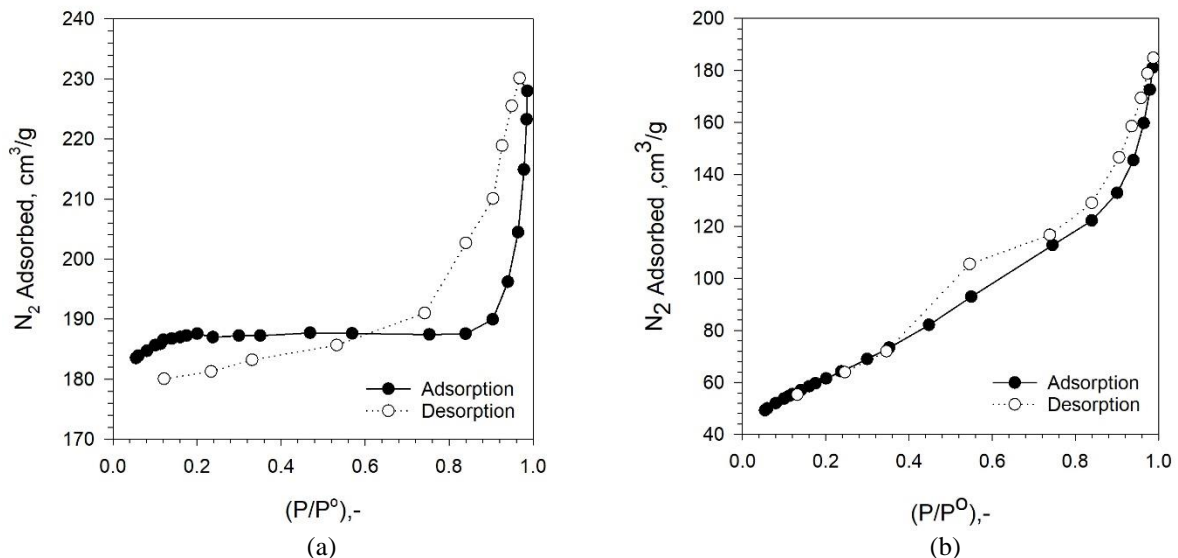


Fig. 1. N_2 Adsorption-desorption Isotherm (a) NaX Zeolite (b) FeX.

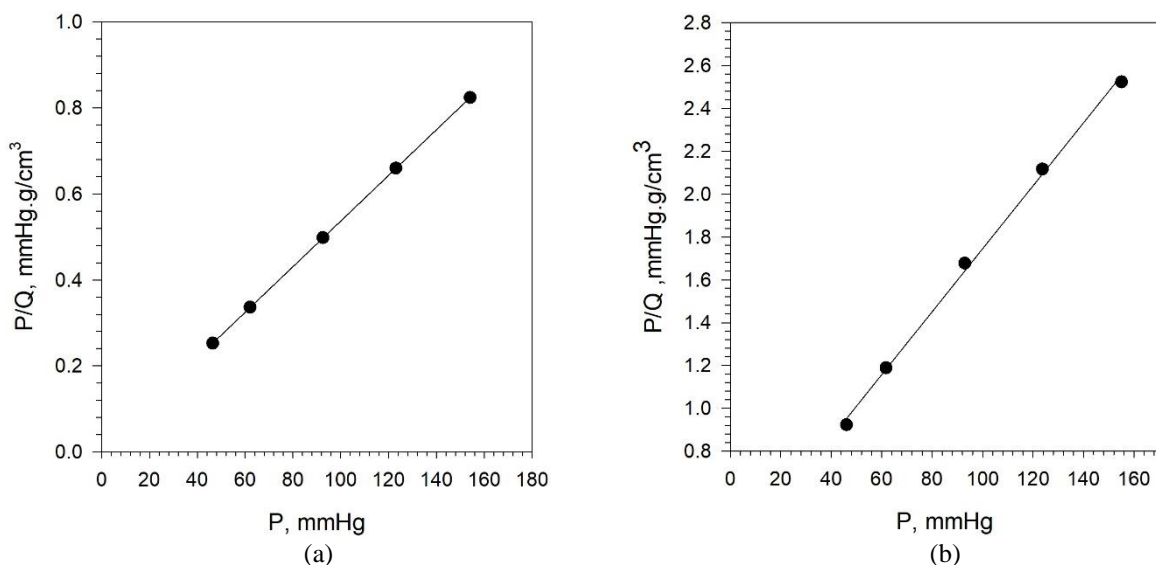


Fig. 2. N_2 Adsorption Isotherm by Langmuir Model (a) NaX Zeolite (b) FeX.

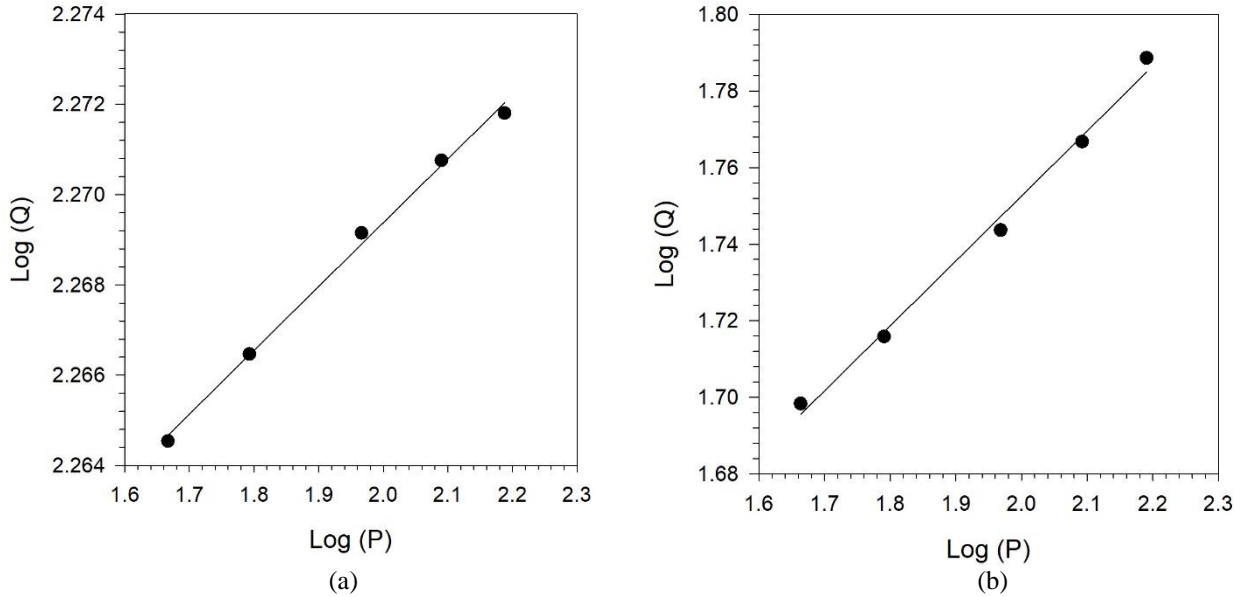


Fig. 3. N₂ Adsorption Isotherm via Freundlich Model (a) NaX Zeolite (b) FeX

Table 1. The Parameters and R² for the Isotherm Models

Isotherm model		NaX zeolite	FeX
Langmuir	Q _m (cm ³ /g)	188.39	68.05
	K _L (1/mm Hg)	47.4369	2.9932
	R ²	0.9999	0.9978
Freundlich	K _F	167.5328	25.9059
	n	70.9219	5.5862
	R ²	0.9961	0.9929
BET	Q _m (cm ³ /g)	130.6585	48.9753
	C	-45.97	762.33
	R ²	0.9914	0.9996

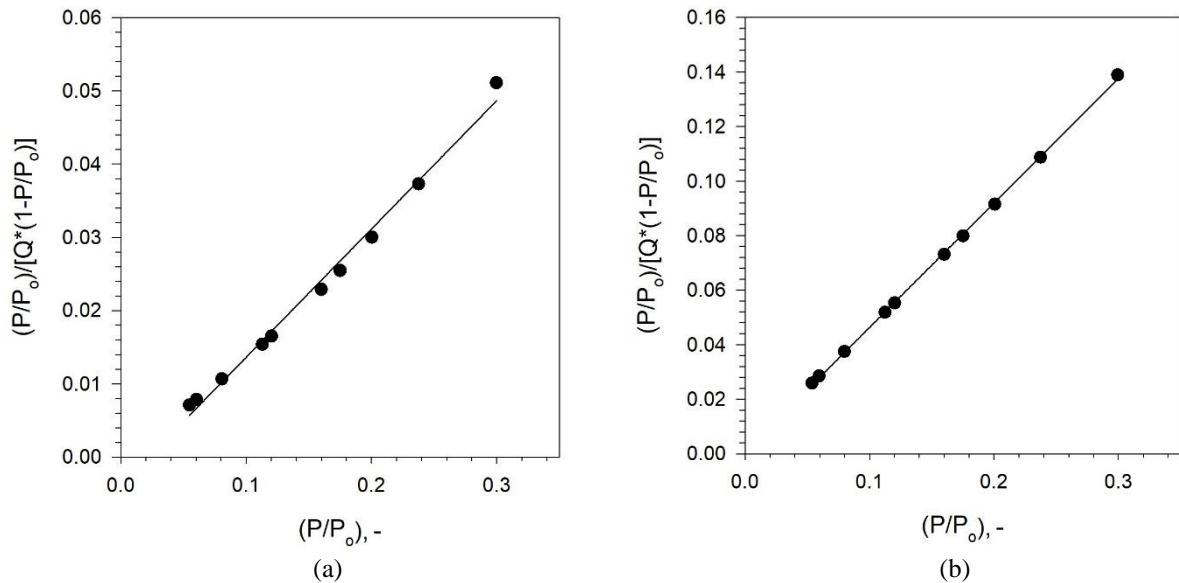


Fig. 4. N₂ Adsorption Isotherm via BET (a) NaX Zeolite (b) FeX.

Textural parameters were compared and summarized in Table 2 for zeolite and FeX, as well as various properties for mesoporous with the same porous structure described in earlier studies [30,44-46]. The surface area of the current NaX was 569.14 m²/g, which was comparable to NaX [30,44-46]. However, the surface area of the present FeX was 213.31 m²/g, which was similar to the surface

area of the Fe-zeolite obtained [44] and lower than the stated surface area of Fe₂O₃-13X [46]. The present NaX has a V_p value of 0.34901 cm³/g, greater than the previous work for the NaX [30] and zeolite Y [44]. The current FeX V_p (0.2768 cm³/g) was in the same range as the obtained Fe exchange [44-46].

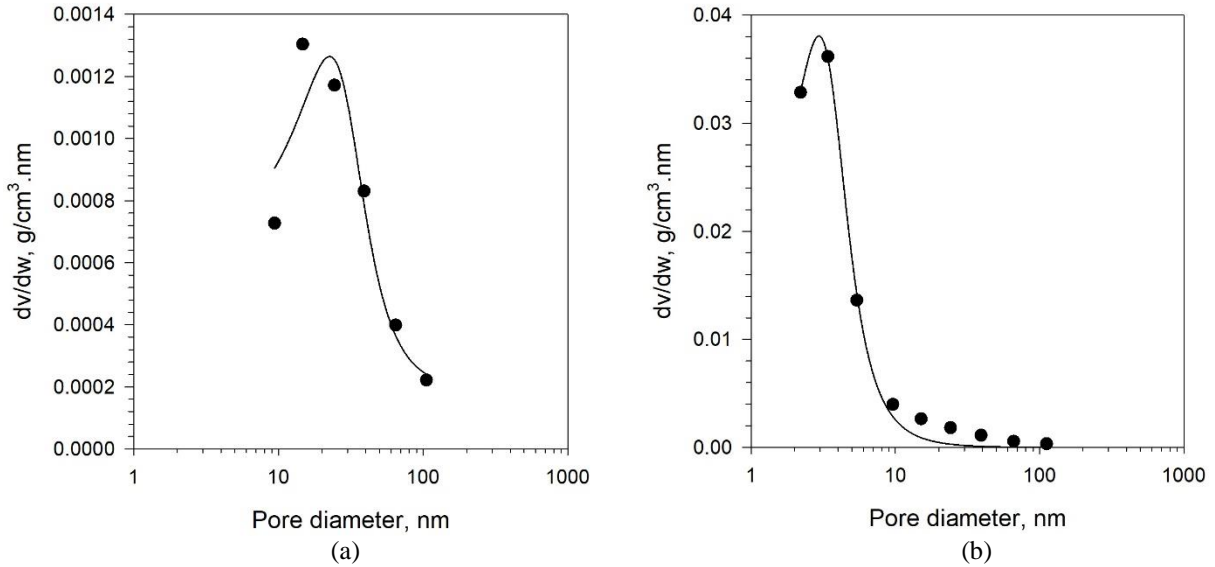


Fig. 5. BJH Particle Size Distribution for (a) NaX Zeolite (b) FeX

Table 2. The Textural Characterization for Various Zeolite Found from N₂ Adsorption at 77.35 K

zeolite	S _{BET} , m ² /g	V _P , cm ³ /g	d _{BJH} , nm	Reference
NaX	569.141	0.3490	2.4529	Current study
NaX	556	0.3270	---	[30]
NaX	573	0.36	2.3	[46]
Zeolite Y	432	0.24	---	[44]
FeX	213.31	0.2768	5.1902	Current study
Fe ₂ O ₃ -13X	541	0.21	2.6	[46]
Fe-zeolite	259	0.10	---	[44]

4- Conclusions

Mixed kinds of I/II isotherms and H3 type hysteresis were noticed in the nitrogen adsorption isotherms on NaX and FeX zeolites according to IUPAC. A more precise pore size may be obtained from the evaluation of an adsorption branch since both micropore and mesopore adsorptions contribute to the adsorption process. The BET isotherm model best represented the experimental results for NaX and FeX zeolites, which had high regression coefficients of R² = 0.9914 and 0.9996, respectively. The BET isotherm model estimated the adsorption capacities of NaX and FeX to be 188.39 cm³/g and 68.05 cm³/g, respectively; the S_{BET} values for NaX and FeX were 569.14 m²/g and 213.31 m²/g. According to the BJH model, NaX pore size distribution was wider than FeX pore size distribution. The d_{BJH} for NaX was 2.4529 nm and 5.1902 nm for FeX, and V_P was 0.3490 cm³/g for NaX and for FeX 0.2768 cm³/g. The comparative research findings between the characteristics and those published suggested that the surface area of NaX and V_P had converged. The comparison findings between the S_{BET} and V_P of FeX equaled and were less than those of FeX.

Nomenclature

Nomenclature	Meaning	Unit
A _m	Adsorption cross-sectional area of the adsorbing species	nm ²

C _{BET}	BET constant	-
C	constant which depends on a curvature equal to 2, in cylindrical shapes	-
d _{BJH}	Pore diameter by BJH	nm
FeX	Fe exchange on NaX zeolite	-
K _f	Freundlich isotherm constant	-
K _L	Langmuir isotherm constant	l/mm Hg
N	Avogadro's number (6.02*10 ²³)	mol ⁻¹
n	Adsorption intensity	-
P	Pressure	mm Hg
P/P ⁰	Relative pressure	-
Q	Nitrogen adsorbed volume at standard pressure and temperature (STP)	cm ³ /g
Q _m	The maximum amount of nitrogen that can be adsorbate to form a monolayer on a solid surface completely	cm ³ /g
r	The liquid's radius of curvature	cm
R	The gas constant	L.mm Hg/mol K

S_{BET}	BET Surface area	m^2/g
S_t	Total surface area	m^2/g
STP	Standard temperature (273 K) and pressure (1 atm)	-
T	Temperature	K
t	Adsorption layer thickness still present on the pores' walls	
V	Nitrogen absorbed molar volume (22.414)	L/mole
v	The condensed adsorptive molar volume	-
V_p	Pore volume	cm^3/g
γ	Liquid surface tension	Dyne/cm
θ	The contact angle between the solid and condensed phase	-

References

- [1] [A. Mhemeed, "A General Overview on the Adsorption," Indian J. Nat. Sci., vol. 9, no. 51, pp. 16127–16131, 2018.](#)
- [2] [P. Panneerselvam, N. Thinakaran, K. V. Thiruvankataravi, M. Palanichamy, and S. Sivanesan, "Phosphoric acid modified-Y zeolites: A novel, efficient and versatile ion exchanger," J. Hazard. Mater., vol. 159, no. 2–3, pp. 427–434, Nov. 2008, doi: 10.1016/j.jhazmat.2008.02.033.](#)
- [3] [D. W. Astuti, Mudasir, and N. H. Aprilita, "Preparation and characterization adsorbent based on zeolite from Klaten, Central Java, Indonesia," J. Phys. Conf. Ser., vol. 1156, no. 1, p. 012002, Jan. 2019, doi: 10.1088/1742-6596/1156/1/012002.](#)
- [4] [I. W. Nah, K.-Y. Hwang, and Y.-G. Shul, "A simple synthesis of magnetically modified zeolite," Powder Technol., vol. 177, no. 2, pp. 99–101, Aug. 2007.](#)
- [5] [A. A. Mohammed and M. K. Baki, "Separation Benzene and Toluene from BTX using Zeolite 13X," Iraqi J. Chem. Pet. Eng., vol. 9, no. 3, pp. 17–22, 2008.](#)
- [6] [A. H. A. K. Mohammed, and M. M. Abdul-Raheem, "Adsorption of BTX Aromatic from Reformate by 13X Molecular Sieve," Iraqi J. Chem. Pet. Eng., vol. 9, no. 4, pp. 13–20, 2008.](#)
- [7] [H. Mousavi, J. Towfighi Darian, and B. Mokhtarani, "Enhanced nitrogen adsorption capacity on \$Ca^{2+}\$ ion-exchanged hierarchical X zeolite," Sep. Purif. Technol., vol. 264, no. September 2020, p. 118442, Jun. 2021, doi: 10.1016/j.seppur.2021.118442.](#)
- [8] [Z. A. Hammood, T. F. Chyad, and R. Al-Saedi, "Adsorption Performance of Dyes Over Zeolite for Textile Wastewater Treatment," Ecol. Chem. Eng. S, vol. 28, no. 3, pp. 329–337, Sep. 2021.](#)
- [9] [S. K. A. Barno, H. J. Mohamed, S. M. Saeed, M. J. Al-Ani, and A. S. Abbas, "Prepared 13X Zeolite as a Promising Adsorbent for the Removal of Brilliant Blue Dye from Wastewater," Iraqi J. Chem. Pet. Eng., vol. 22, no. 2, pp. 1–6, Jun. 2021.](#)
- [10] [T. P. Belova, "Adsorption of heavy metal ions \(\$Cu^{2+}\$, \$Ni^{2+}\$, \$Co^{2+}\$ and \$Fe^{2+}\$ \) from aqueous solutions by natural zeolite," Heliyon, vol. 5, no. 9, p. e02320, Sep. 2019, doi: 10.1016/j.heliyon.2019.e02320.](#)
- [11] [L. F. de Magalhães, G. R. da Silva, and A. E. C. Peres, "Zeolite Application in Wastewater Treatment," Adsorpt. Sci. Technol., vol. 2022, pp. 1–26, Feb. 2022, doi: 10.1155/2022/4544104.](#)
- [12] [E. Erdem, N. Karapinar, and R. Donat, "The removal of heavy metal cations by natural zeolites," J. Colloid Interface Sci., vol. 280, no. 2, pp. 309–314, Dec. 2004, doi: 10.1016/j.jcis.2004.08.028.](#)
- [13] [H. L. Tran, M. S. Kuo, W. D. Yang, and Y. C. Huang, "Study on Modification of NaX Zeolites: The Cobalt \(II\)-Exchange Kinetics and Surface Property Changes under Thermal Treatment," J. Chem., vol. 2016, no. II, 2016, doi: 10.1155/2016/1789680.](#)
- [14] [E. Asedegbega-Nieto, E. Díaz, A. Vega, and S. Ordóñez, "Transition metal-exchanged LTA zeolites as novel catalysts for methane combustion," Catal. Today, vol. 157, no. 1–4, pp. 425–431, Nov. 2010, doi: 10.1016/j.cattod.2010.05.032.](#)
- [15] [E. V. Kuznetsova, E. N. Savinov, L. A. Vostrikova, and V. N. Parmon, "Heterogeneous catalysis in the Fenton-type system \$FeZSM-5/H_2O_2\$," Appl. Catal. B Environ., vol. 51, no. 3, pp. 165–170, Aug. 2004, doi: 10.1016/j.apcatb.2004.03.002.](#)
- [16] [B. A. Alshahidy and A. S. Abbas, "Comparative Study on the Catalytic Performance of a 13X Zeolite and its Dealuminated Derivative for Biodiesel Production," Bull. Chem. React. Eng. Catal., vol. 16, no. 4, pp. 763–772, Dec. 2021, doi: 10.9767/bcrec.16.4.11436.763-772.](#)
- [17] [B. A. Alshahidy and A. S. Abbas, "Preparation and modification of 13X zeolite as a heterogeneous catalyst for esterification of oleic acid," AIP Conf. Proc., vol. 2213, no. March, 2020.](#)
- [18] [A. Gęsikiewicz-Puchalska et al., "Changes in porous parameters of the ion exchanged x zeolite and their effect on \$CO_2\$ adsorption," Molecules, vol. 26, no. 24, 2021, doi: 10.3390/molecules26247520.](#)
- [19] [Y. Zeng, "Fundamental Study of Adsorption and Desorption Process in Porous Materials with Functional Groups," p. 122, 2016.](#)
- [20] [M. Alaqarbeh, "Adsorption Phenomena : Definition , Mechanisms , and Adsorption Types : RHAZES : Green and Applied Chemistry Adsorption Phenomena : Definition , Mechanisms , and Adsorption Types : Short Review," no. September, 2021, doi: 10.48419/IMIST.PRSM/rhazes-v13.28283.](#)
- [21] [R. T. Yang, "Adsorbents: Fundamentals and Applications," Wiley-Interscience, 2003.](#)
- [22] [S. M. Gawande, N. S. Belwalkar, and A. A. Mane, "Adsorption and its Isotherm – Theory," Int. J. Eng. Res., vol. 6, no. 6, p. 312, 2017, doi: 10.5958/2319-6890.2017.00026.5.](#)
- [23] [G. F. Bennett, Partition and Adsorption of Organic Contaminants in Environmental Systems, vol. 98, no. 1–3, 2003.](#)

- [24] [M. A. Al-Ghouti and D. A. Da'ana, "Guidelines for the use and interpretation of adsorption isotherm models: A review," J. Hazard. Mater., vol. 393, no. February, p. 122383, Jul. 2020, doi: 10.1016/j.jhazmat.2020.122383.](#)
- [25] [M. Thommes et al., "Physisorption of gases, with special reference to the evaluation of surface area and pore size distribution \(IUPAC Technical Report\)," Pure Appl. Chem., vol. 87, no. 9–10, pp. 1051–1069, 2015, doi: 10.1515/pac-2014-1117.](#)
- [26] [K. Sing, "The use of nitrogen adsorption for the characterisation of porous materials," Colloids Surfaces A Physicochem. Eng. Asp., vol. 187–188, pp. 3–9, Aug. 2001, doi: 10.1016/S0927-7757\(01\)00612-4.](#)
- [27] [B. Kurji, A. Abbas, and I. Marshes Research Center, "Comparative Study of Textural Properties for Various Silica by Nitrogen Adsorption-desorption Technique," Egypt. J. Chem., 2022, doi: https://dx.doi.org/10.21608/ejchem.2022.125169.5568.](#)
- [28] [A. I. Moral-Rodríguez et al., "Tailoring the textural properties of an activated carbon for enhancing its adsorption capacity towards diclofenac from aqueous solution," Environ. Sci. Pollut. Res. Int., vol. 26, no. 6, pp. 6141–6152, Feb. 2019, doi: 10.1007/s11356-018-3991-x.](#)
- [29] [M. N. Alaya, a M. Youssef, M. Karman, and H. E. A. El-aal, "Textural properties of Activated Carbons from Wild Cherry Stones as Determined by Nitrogen and Carbon Dioxide Adsorption," vol. 7, no. 1, pp. 9–18, 2006.](#)
- [30] [H. Hammoudi, S. Bendenia, K. Marouf-Khelifa, R. Marouf, J. Schott, and A. Khelifa, "Effect of the binary and ternary exchanges on crystallinity and textural properties of X zeolites," Microporous Mesoporous Mater., vol. 113, no. 1–3, pp. 343–351, Aug. 2008, doi: 10.1016/j.micromeso.2007.11.032.](#)
- [31] [I. Langmuir, "The constitution and fundamental properties of solids and liquids. Part II.-Liquids," J. Franklin Inst., vol. 184, no. 5, p. 721, 1917, doi: 10.1016/s0016-0032\(17\)90088-2.](#)
- [32] [J. H. De Boer, "Adsorption Phenomena," in Physical Chemistry of Solid-Gas Interfaces, London, UK: ISTE, 1956, pp. 1–27.](#)
- [33] [H. Zhang, A. Goepfert, S. Kar, and G. K. S. Prakash, "Structural parameters to consider in selecting silica supports for polyethylenimine based CO₂ solid adsorbents. Importance of pore size," J. CO₂ Util., vol. 26, pp. 246–253, Jul. 2018, doi: 10.1016/j.jcou.2018.05.004.](#)
- [34] [B. H. Hameed, D. K. Mahmoud, and A. L. Ahmad, "Equilibrium modeling and kinetic studies on the adsorption of basic dye by a low-cost adsorbent: Coconut \(Cocos nucifera\) bunch waste," J. Hazard. Mater., vol. 158, no. 1, pp. 65–72, Oct. 2008, doi: 10.1016/j.jhazmat.2008.01.034.](#)
- [35] [K. Y. Foo and B. H. Hameed, "Insights into the modeling of adsorption isotherm systems," Chem. Eng. J., vol. 156, no. 1, pp. 2–10, Jan. 2010.](#)
- [36] [P. M. V. Raja and A. R. Barron, "BET surface area analysis of nanoparticles," Phys. Methods Chem. Nano Sci., vol. i, pp. 1–7, 2019.](#)
- [37] [E. Sugawara and H. Nikaido, "Properties of AdeABC and AdeIJK efflux systems of Acinetobacter baumannii compared with those of the AcrAB-TolC system of Escherichia coli," Antimicrob. Agents Chemother., vol. 58, no. 12, pp. 7250–7, Dec. 2014, doi: 10.1128/AAC.03728-14.](#)
- [38] [M. Thommes, "Physical adsorption characterization of nanoporous materials," Chemie-Ingenieur-Technik, vol. 82, no. 7, pp. 1059–1073, 2010, doi: 10.1002/cite.201000064.](#)
- [39] [A. Marcilla, A. Gomez-Siurana, M. M. José, and F. J. Valdés, "Comments on the Methods of Characterization of Textural Properties of Solids from Gas Adsorption Data," Adsorpt. Sci. Technol., vol. 27, no. 1, pp. 69–84, Feb. 2009, doi: 10.1260/026361709788921579.](#)
- [40] [B. X. Medina-Rodríguez and V. Alvarado, "Use of Gas Adsorption and Inversion Methods for Shale Pore Structure Characterization," Energies, vol. 14, no. 10, p. 2880, May 2021, doi: 10.3390/en14102880.](#)
- [41] [E. P. Barrett, L. G. Joyner, and P. P. Halenda, "The Determination of Pore Volume and Area Distributions in Porous Substances. I. Computations from Nitrogen Isotherms," J. Am. Chem. Soc., vol. 73, no. 1, pp. 373–380, 1951, doi: 10.1021/ja01145a126.](#)
- [42] [D. Dollimore and G. R. Heal, "Pore-size distribution in typical adsorbent systems," J. Colloid Interface Sci., vol. 33, no. 4, pp. 508–519, 1970, doi: 10.1016/0021-9797\(70\)90002-0.](#)
- [43] [S. Geraedts, "Pore size distribution and surface group analysis a study of two electrical grade carbon blacks," Eindhoven Univ. Technol., 2002.](#)
- [44] [M. L. Rache, A. R. García, H. R. Zea, A. M. T. Silva, L. M. Madeira, and J. H. Ramírez, "Azo-dye orange II degradation by the heterogeneous Fenton-like process using a zeolite Y-Fe catalyst—Kinetics with a model based on the Fermi's equation," Appl. Catal. B Environ., vol. 146, pp. 192–200, Mar. 2014, doi: 10.1016/j.apcatb.2013.04.028.](#)
- [45] [S. K. Kamal, A. S. Abbas "Langmuir-Hinshelwood-Hougen-Watson Heterogeneous Kinetics Model for the Description of Fe \(II \) Ion Exchange on Na-X Zeolite," Eng. Technol. Appl. Sci. Res., vol. 12, no. 5, pp. 9265–9269, 2022.](#)
- [46] [A. A. AbdulRazak and S. Rohani, "Sodium Dodecyl Sulfate-Modified Fe₂O₃/Molecular Sieves for Removal of Rhodamine B Dyes," Adv. Mater. Sci. Eng., vol. 2018, pp. 1–10, 2018, doi: 10.1155/2018/3849867.](#)

توصيف الخصائص التركيبية لزيوليت NaX و Fe-X بواسطة تقنية امتصاص-امتزاز النيتروجين

سناريا كامل كمال و عمار صالح عباس

جامعة بغداد /كلية الهندسة /قسم الهندسة الكيميائية

الخلاصة

للخصائص التركيبية للزيوليت تأثير كبير على فعالية الزيوليت في العمليات الصناعية المختلفة. يهدف هذا البحث إلى دراسة الخصائص النصية لزيوليت NaX و FeX باستخدام تقنية امتصاص النيتروجين-الامتصاص عند درجة حرارة منخفضة ثابتة. وفقاً للاتحاد الدولي للكيمياء البحتة والتطبيقية ، أظهر متساوي الامتصاص والامتصاص أن المواد المدروسة كانت مختلطة من النوعين I / II متساوي الحرارة ونوع H3. كانت متساوي الحرارة Brunauer–Emmett–Teller أفضل نموذج لوصف امتزاز وامتصاص النيتروجين بشكل أفضل من متساوي الحرارة Langmuir و Freundlich. كانت سعة الامتزاز التي تم الحصول عليها وقيم مساحة سطح Brunauer–Emmett–Teller لـ NaX أكبر من تلك الخاصة بـ FeX. وفقاً لمعادلة كلفن، تم استخدام نموذج Halenda و Joyner و Barrett لتحديد توزيع حجم المسام والقطر ومتوسط حجم المسام للزيوليت المختارة. كان توزيع حجم المسام لـ NaX أوسع من زيوليت FeX، وكان قطر المسام لـ NaX أقل من FeX، وكان متوسط حجم المسام لـ FeX أكبر من قيمة متوسط حجم مسام NaX. أجريت الدراسة المقارنة مع الدراسات السابقة، وأظهرت المقارنة أن الخصائص النصية للزيوليت المعدلة تتفق مع الدراسات الأخرى.

الكلمات الدالة: التبادل الأيوني، ميزوبوروس، متساوي الحرارة، مساحة السطح، توزيع حجم المسام، قطر المسام، متوسط حجم المسام.